Coin tossing as a billiard problem

N. L. Balazs, Rupak Chatterjee, and A. D. Jackson
Department of Physics, State University of New York at Stony Brook, Stony Brook, New York 11794-3800
(Received 17 February 1995)

We demonstrate that the free motion of any two-dimensional rigid body colliding elastically with two parallel, flat walls is equivalent to a billiard system. Using this equivalence, we analyze the integrable and chaotic properties of this class of billiards. This provides a demonstration that coin tossing, the prototypical example of an independent random process, is a completely chaotic (Bernoulli) problem. The related question of which billiard geometries can be represented as rigid body systems is examined.

PACS number(s): 05.45.+b

I. INTRODUCTION

Classical dynamics can describe chaotic motion. It is generally accepted that truly chaotic systems are isomorphic to Bernoulli systems. This means that any chaotic solution is equivalent in a well-defined sense to a stochastic one generated by an independent random process. The prototype of such a process is coin tossing described by repeated random trials with only two possible outcomes for each trial with probabilities which do not change during the trials. These trials are called Bernoulli trials, hence the name. However, the tossing of a coin can also be viewed as a simple dynamical system since it is merely the motion of a rigid body subjected to simple forces and boundary conditions. It is legitimate to ask whether coin tossing is *de facto* a Bernoulli system when considered as a dynamical process. The experience of gamblers through the ages would suggest that it is. The aim of the present paper is to provide a more mathematical demonstration.

To be specific, we shall consider a rigid body in two dimensions which moves in the absence of forces and makes elastic collisions with two infinitely massive parallel walls. The special case in which this rigid body is simply a stick of zero width will serve to model coin tossing. We shall demonstrate that this system is equivalent to that of a point particle colliding with a suitably curved wall. The key feature to this equivalence is the fact that elastic collisions by the rigid body necessarily imply *specular* reflections for the related point particle, i.e., the behavior of a traditional billiard. For the special case of tossing a coin between plane walls, the equivalent billiard configuration is that of a particle bouncing between two convex sinusoidal boundary walls. It has been shown in [1] that billiards with strictly convex walls are of the Bernoulli type indicating that coin tossing, when considered as a dynamical system, is truly a completely random process. However, for billiards arising from coin tossing, the correlation between the initial orientation of the coin and its orientation on subsequent bounces dies out with an exponential envelope. This then provides a characteristic decorrelation time after which the process is random. A fair coin toss must necessarily allow the coin to bounce repeatedly on the floor and the ceiling. Evidently, a simple toss and catch process, the colloquial example of a random process, does not suffice.

We shall see that every such rigid body system is equivalent to a unique billiard problem. The generality of this equivalence is of some interest. For some time, billiard problems have been known to provide convenient and illustrative examples of the general properties of Hamiltonian dynamical systems [2–4]. The quantum properties of billiards have also been studied (see, for instance, [5]). Physical realizations of billiard systems have been found in microwave cavities as well as in electronic nanometric semiconductor devices and used to investigate how the transition from regular to chaotic motion influences the wave properties of these systems [6–8]. Yet, many of the billiard geometries studied are somewhat arbitrary and do not represent real physical systems. The present results offer a broad class of physically realizable dynamical systems exhibiting all types of motion; integrable, near integrable (KAM), and chaotic motion of increasing randomness (K flows, C flows, and Bernoulli flows).

The organization of the paper is as follows. In Sec. II, we consider the specific problem of the stick (or coin). The general transformations relating the rigid body problem to the billiard system are derived, and the condition for specular reflection is proved. Section III deals with some of the properties associated with elliptical rigid bodies. In particular, we consider how the onset of chaos depends on the eccentricity of the ellipse and the separation between the walls. In Sec. IV, we consider the inverse problem of deriving body shapes from given wall shapes. Finally, a number of conclusions are drawn in Sec. V along with some suggestions for certain interesting shapes and possible directions for a quantum-mechanical analysis of this problem.

II. TRANSFORMATION EQUATIONS

A. Sticks

Let us first consider the simple case of a stick of length $2L$, mass M, and radius of gyration κ, bouncing freely between two flat walls separated by a distance H. (For simplicity, we assume that the center of mass is at the

midpoint of the stick.) The position of the stick is characterized by y, the height of the center of mass above the lower wall, and θ, the angle of rotation of the stick from the vertical. If we introduce the dimensionless height $\eta = y/\kappa$, the (scaled) energy of the stick is given by

$$E = \frac{M}{2}(\dot{\theta}^2 + \dot{\eta}^2). \tag{1}$$

This looks formally like the energy of a free point particle moving in an Euclidean plane parametrized by the dimensionless coordinates $x_1 = \theta$ and $x_2 = \eta$. At the collision of the stick with the wall, it is easy to see that

$$\begin{aligned}(M\kappa)\delta\dot{\eta} &= f_n \delta t,\\ (M\kappa^2)\delta\dot{\theta} &= L\sin(\theta) f_n \delta t,\end{aligned} \tag{2}$$

where f_n is the normal force at the wall. This gives a linear relation between the change in velocities at the collision point,

$$\delta\dot{\theta} = \frac{L}{\kappa}\sin(\theta)\delta\dot{\eta}. \tag{3}$$

Now, the boundary for the motion of our point particle is given by the minimum value of η for a given angular orientation. From conservation of energy we find [using (1) and (3)] that

$$\delta\dot{\eta} = \frac{-2[\dot{\eta} + (L/\kappa)\dot{\theta}\sin(\theta)]}{1 + (L/\kappa)^2\sin(\theta)^2}, \tag{4}$$

resulting in $\eta_{\min} = (L/\kappa)|\cos(\theta)|$. Therefore, the bottom and top boundary walls [$b(\theta)$ and $t(\theta)$, respectively] corresponding to the billiard problem for the stick are

$$\begin{aligned}b(\theta) &= \frac{L}{\kappa}|\cos(\theta)|,\\ t(\theta) &= H - \frac{L}{\kappa}|\cos(\theta)|.\end{aligned} \tag{5}$$

Finally, consider the infinitesimal change in the velocity vector of our point particle after a collision,

$$\delta\vec{v} = (\vec{T}\cdot\delta\vec{v})\vec{T} + (\vec{N}\cdot\delta\vec{v})\vec{N}. \tag{6}$$

Here, $\vec{T}$ and $\vec{N}$ are the orthonormal tangent and normal vectors at the billiard boundary. The tangent vector along the lower wall is

$$\vec{T} = \left(1, -\frac{L}{\kappa}\sin(\theta)\right). \tag{7}$$

Using (3), we have

$$\vec{T}\cdot\delta\vec{v} = \vec{T}\cdot(\delta\dot{\theta}, \delta\dot{\eta}) = 0, \tag{8}$$

and consequently, the tangential component of $\delta\vec{v}$ vanishes. Since the magnitude of $\vec{v}$ is preserved by energy conservation, the above result indicates that upon collision, the normal component of $\vec{v}$ simply changes sign. Thus, the point particle in our equivalent billiard undergoes *specular* reflections at the boundary walls. Hence, the motion of a rigid stick is equivalent to a billiard problem with properly chosen boundaries. (Since the horizontal θ axis is clearly periodic, one may consider the configuration space to be the surface of a cylinder with "undulating" top and bottom edges.)

B. Arbitrary shapes and mass distributions

It is a simple matter to generalize the above to the case of rigid bodies of arbitrary shape. We restrict our discussion to objects possessing at least one symmetry axis in the plane. (The procedure for asymmetric objects is identical except that the upper boundary is shifted by π with respect to the lower one.) Consider a closed plane curve $\mathcal{C}$. If $\mathcal{C}$ is not everywhere convex, we replace $\mathcal{C}$ with its convex envelope since concave segments cannot come into contact with the boundary walls. As before, the inertial properties of the object will be expressed in terms of the total mass M and the radius of gyration κ. The height of the center of mass of the object above the wall will be denoted by η (scaled by the gyration factor κ). The curve $\mathcal{C}$ can be specified completely by its radius, $R(\alpha)$, as a function of the angle α from some body-fixed axis $\hat{a}$,

$$\vec{R}(\alpha) = (R(\alpha)\cos(\alpha), R(\alpha)\sin(\alpha)). \tag{9}$$

It is elementary to construct the tangent to $\mathcal{C}$, defined as

$$\vec{T}(\alpha) = d\vec{R}/d\alpha \ , \tag{10}$$

and the associated normal vector $\vec{N}(\alpha)$. When the point of contact between the body and the wall is at α_c, the perpendicular distance between the center of mass and the wall is simply

$$b(\alpha_c) = \frac{1}{\kappa}\frac{\vec{N}\cdot\vec{R}}{(\vec{N}\cdot\vec{N})^{1/2}} = \frac{1}{\kappa}\frac{R^2}{\sqrt{R^2 + R'^2}} \ . \tag{11}$$

To obtain the desired wall shape, we must determine that orientation of the rigid body, θ, which makes α_c the point of contact. (For convenience, we measure θ, clockwise, from the normal to the bottom wall to the body-fixed axis $\vec{a}$.) Obviously, the condition of tangency is that $\vec{N}(\alpha_c)$ is parallel to the wall normal:

$$\frac{R'(\alpha_c)}{R(\alpha_c)} = \tan(\alpha_c + \theta), \tag{12}$$

which then produces the lower boundary $b(\theta) = b(\alpha_c(\theta))$ with the upper wall being given by $t(\theta) = H - b(\theta)$ [or $t(\theta) = H - b(\theta + \pi)$ for asymmetric objects].

The equations describing the actual collision have a form similar to Eqs. (2),

$$\begin{aligned}(M\kappa)\delta\dot{\eta} &= f_n \delta t,\\ (M\kappa^2)\delta\dot{\theta} &= R(\alpha_c)\sin(\alpha_c + \theta) f_n \delta t,\end{aligned} \tag{13}$$

with the energy again being given by (1). Since Eq. (13) follows from (2) with the substitutions

$$L \to R(\alpha_c) \ ,$$
$$\theta \to \theta + \alpha_c \ , \tag{14}$$

it is clear that the proof for specular reflection is identical to that given for the stick. Thus, for *every* shape of the rigid body, there is an equivalent billiard problem.

As an example of the above procedure, consider an elliptical disk with a semimajor axis of 1 and a semiminor axis of $1/(\sqrt{1+\epsilon})$. Imagine that the center of mass is at the geometric center of the ellipse. Relative to this point, the ellipse is parametrized as

$$R(\alpha) = \frac{1}{[1+\epsilon \sin^2(\alpha)]^{1/2}}. \tag{15}$$

Equation (12) leads to

$$\cos(\alpha_c + \theta) = \frac{[1+\epsilon \sin^2(\alpha_c)]}{[1+(\epsilon^2+2\epsilon)\sin^2(\alpha_c)]^{1/2}} \tag{16}$$

and

$$\sin^2(\alpha_c) = \frac{\sin^2(\theta)}{[1+(\epsilon^2+2\epsilon)\cos^2(\theta)]}. \tag{17}$$

Substituting (15), (16), and (17) into (11) and (12) results in the following billiard boundary:

$$b(\theta) = \left(\frac{1}{\kappa}\right)\sqrt{\frac{[1+\epsilon\cos^2(\theta)]}{1+\epsilon}}. \tag{18}$$

In the limit of $\epsilon \to 0$, $b(\theta) \to 1/\kappa$ which is the obvious result for a circle of radius 1. In the other limit $\epsilon \to \infty$, the ellipse degenerates into a stick and we recover the previous result of $b(\theta) = (1/\kappa)|\cos(\theta)|$.

III. ELLIPTIC DISKS

A. KAM motion

We now focus on the special case in which the rigid body is an ellipse so that the equivalent billiard problem has the wall described by Eq. (18) of the preceding section. A Poincaré section map for the elliptic system with $\epsilon = 0.03$ and $H = 3$ is shown in Fig. 1. This is a phase portrait of the contact point θ_c versus the angle of incidence ϕ_c with respect to the local normal at θ_c. The regular and chaotic regions of this "mixed" system are clearly visible. For such a small value of the eccentricity ϵ, the boundary can be expanded as

$$b(\theta) \simeq [1 - (\epsilon/2)\sin^2(\theta)]. \tag{19}$$

This indicates that even a small variation from the integrable billiard generated by a circle can produce a dense population of stochastic trajectories. The corresponding phase space can be described using the KAM theorem [9]. For instance, Fig. 2 is a phase portrait for $\epsilon = 0.55$ and $H = 1.9$. This section map contains both hyperbolic and elliptical regions of phase space. The inner circles

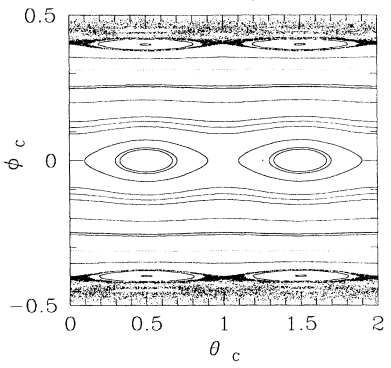

FIG. 1. Phase portrait (in units of π) of the contact point θ_c versus the angle of incidence ϕ_c with respect to the local normal θ_c for the elliptic system $\epsilon = 0.03$ and $H = 3$.

correspond to KAM tori of irrational winding number frequencies. The island chains encircling these tori surround the elliptic fixed points of the motion. As is well known, this structure persists at smaller length scales.

The transition from a mixed geometry to a chaotic one occurs suddenly in these rigid body problems. As long as the motion is purely chaotic, the actual value of H plays no explicit role. When the motion contains both hyperbolic and elliptic regions, the relative size of these different regions is dictated by the height H with the elliptic regions disappearing as H and/or ϵ become larger. It is somewhat delicate to make a numerical determination of the curve which separates the KAM and chaotic regions. This is particularly true when H is large and ϵ is small. The approximate boundary curve for the elliptic problem is

$$\epsilon \simeq \frac{1}{H} + \frac{17}{H^2} \ . \tag{20}$$

This expression reproduces the results of simulations to about 1% which is probably the limit of their accuracy. In the limit as $\epsilon \to 0$ and the object approaches a circle, the wall function approaches a constant plus a small

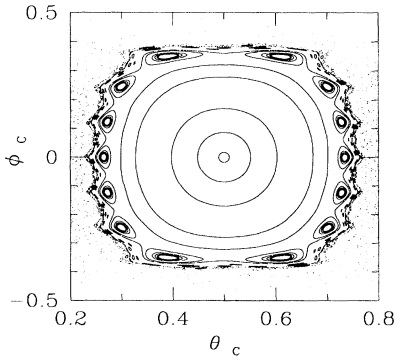

FIG. 2. Phase space diagram for the billiard system with $\epsilon = 0.55$ and $H = 1.9$.

sinusoidal oscillation. Given any ϵ, Eq. (20) shows us that it is always possible to pick H sufficiently large that K-type motion results.

B. Application to coins

The case of a very eccentric ellipse can be viewed as a model of a coin tossing process. Regarding this ellipse as a coin observed edgewise, we place an oriented arrow along its length. With this fixed orientation, we assign the condition "heads" when the arrow points to the right and "tails" when the arrow points to the left. The motion of the coin consists of the one-dimensional vertical motion of the center of mass and a superimposed rotation. This leads to a strictly convex billiard problem $b(\theta) = |\cos(\theta)|$ which has been shown [1] to be isomorphic to a Bernoulli shift. Surprisingly, this includes the case where the distance between the walls is less than the length of the stick. (In our coin analogy, this means that the room is not high enough to permit the coin to flip from heads to tails.) In this case, the full angular region is not accessible. Nevertheless, the motion is chaotic. This is consistent with Eq. (20), which indicates that, for any H, it is always possible to pick ϵ sufficiently large that K-type motion results.

In spite of its common use as a random process, the traditional tossing of a coin (without bounces) is nothing of the sort. As we have shown, the present coin toss (including collisions with a wall) does result in K-type motion. It is thus of some interest to consider the probability $P(n)$ that, if the coin shows a "head" at a given collision with the bottom wall, it will also show a "head" n collisions later. (To be precise, we count only collisions with the bottom wall which have been preceded by a collision with the top wall.) We expect $P(n) \to 1/2$ for an independent random process. We have studied $P(n)$ numerically for several values of H for an ellipse of large eccentricity ($\epsilon = 99$). The resulting values of $|P(n)-1/2|$ are shown in Fig. 3 for wall separations which are 5%, 10%, and 15% larger than the length of the stick. Since we expect K-type motion for these values of H and ϵ, we studied $P(n)$ by following a number (10 to 20) of long trajectories (of roughly 10^5 collisions each). The spread in the results was used to estimate the uncertainty in $P(n)$. It is apparent from Fig. 3 that $P(n)$ approaches the asymptotic value of 1/2 exponentially and is well-described by

$$P(n) - 1/2 \approx 1/2 \exp(-n/\tau(H)). \tag{21}$$

Although $[P(n) - 1/2]$ is a positive and monotonically decreasing function for the values of n shown in Fig. 3, we cannot exclude the possibility of small oscillations for larger values of n. There is certainly a region of somewhat larger wall separations for which $[P(n) - 1/2]$ is clearly negative for small n. The safest conclusion is that $[P(n)-1/2]$ is probably bounded by an exponential envelope. When the distance between the walls is (less than or) equal to the diameter of the coin, the correlation time is evidently infinite. As the wall separation is increased slightly, the correlation time is approximately inversely proportional to the difference between H and the diameter of the coin. It is technically challenging to follow this H dependence numerically for larger separations (or for significantly more time steps than shown in Fig. 3) since the correlations decay so rapidly. This exponential-like decay is not unexpected (many results on billiard correlation functions have been found for other billiard systems; see, for instance, [10]). When the wall separation is only slightly larger than the size of the coin, the wall function reveals a long and narrow neck between "heads" and "tails" regions. The probability of a successful transition is small. On average, the coin will undergo a large number of collisions while traversing the neck. Small changes in the trajectory on entry will result in large changes in the trajectory when it emerges. Motion in the "heads" and "tails" sectors will be largely uncorrelated, and the exponential decay seen in Fig. 3 is not unreasonable. "House rules" at casinos inevitably require that dice be bounced from a wall. The present results suggest that this bounce plays a significant role in randomizing the outcome and is not merely a time-honored tradition.

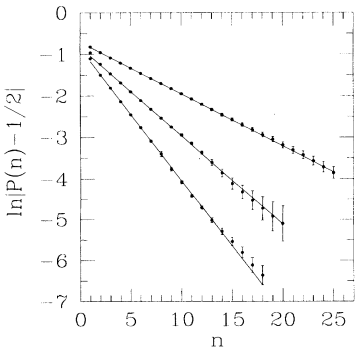

FIG. 3. Exponentially decaying correlation functions for the stretched ellipse $\epsilon = 99$ and wall separations $H = 2.3$ (lower line), $H = 2.2$ (middle line), and $H = 2.1$ (upper line).

IV. FROM WALL SHAPES TO BODY SHAPES

We have demonstrated that every problem involving elastic collisions between a rigid body and parallel walls is equivalent to a billiard with a suitable (and unique) choice of the wall function $b(\theta)$. Here, we wish to address the inverse problem. For convenience, we shall restrict our attention to periodic walls which are everywhere differentiable. (This is not to deny that rigid bodies with sharp corners are also of interest.) There are several questions of interest: How does one determine $R(\alpha)$ given $b(\theta)$? Does every periodic $b(\theta)$ correspond to a realizable rigid body and, if so, is its shape unique? The general technique for going from $b(\theta)$ to $R(\alpha)$ is easy to state but can be challenging to implement. Formally, we use Eq. (12) to eliminate θ from Eq. (11). This leads to a nonlinear but first-order differential equation for $R(\alpha)$. Two observations are useful. First, the extrema in b (as a

function of θ) coincide with the extrema of R (as a function of α) with α and θ related by Eq. (12). Second, at such extrema, $\alpha = \theta$ and $R(\alpha) = b(\theta)$. While it may be difficult to find analytic solutions to the resulting equation, numerical solutions are accessible. It is not always easy to find them. For example, imagine that the wall shape is given by Eq. (17). The procedure stated leads to a quadratic equation for $R'(\alpha)$ which is readily solved to yield

$$\frac{R'}{R} = \frac{-\epsilon \sin\alpha \cos\alpha \pm \sqrt{-1-\epsilon+(1+\epsilon)(1+\epsilon\sin^2\alpha)R^2}}{1+\epsilon\sin^2\alpha} \tag{22}$$

which is consistent with Eq. (15). Note, however, this consistency is realized by two degenerate solutions which render the numerical problem delicate.

As we shall see, every periodic $b(\theta)$ can be regarded as an equivalent rigid body problem. According to a well-known theorem, $b(\theta)$ must have at least four extrema to represent a physical wall shape. Every nonconstant, periodic function must have at least one maximum and one minimum. Thus, the four-extremum requirement can always be met by mapping $\theta \to \theta/2$. Before proceeding, we note a fundamental ambiguity in the inverse problem. If one is given only the equivalent billiard problem, the distinction between $b(\theta)$ and H, the separation between the parallel walls, cannot be made uniquely. Thus, $b(\theta)$ can only be determined up to some constant shift b_0. Due to the nonlinear nature of the inverse problem, the corresponding $R(\alpha)$ generally depends on the value of b_0 assumed. Hence, the equivalent billiard does not determine the rigid body uniquely. Moreover, there will generally be choices of b_0 for which no physically realizable $R(\alpha)$ exists. (The specific example of elliptic disks is considered in the Appendix where we show that no physical solution exists when b_0 is less than some critical value.)

While the freedom of choosing b_0 and the associated multiplicity of body shapes which arise from its exploitation may seem unfortunate, there is a positive side. This freedom allows us to see that there are always (infinitely many) rigid body shapes corresponding to any choice of $b(\theta)$. Proof of existence is compensation for loss of uniqueness. Consider the elliptic example for large, positive b_0 so that θ-dependent contributions to the wall function are small relative to b_0. The angles α and θ are almost equal, and the resulting body is almost a circle. For sufficiently large b_0, this will hold for all $b(\theta)$. Then,

$$b_0 + b\left(\alpha + \tan^{-1}\left(\frac{R'}{R}\right)\right) = \frac{R^2}{\sqrt{R^2+R'^2}} \tag{23}$$

with

$$R = b_0 + r(\alpha) \ . \tag{24}$$

It is understood that $b_0 \gg r$. This inequality entitles us to expand Eq. (23) in powers of r/b_0 and r'/b_0 which yields

$$\alpha = \theta, \qquad R(\alpha) = b_0 + b(\alpha) \ . \tag{25}$$

Further, by considering Eq. (A3), we see that the curvature of this shape will always be positive for sufficiently large b_0 independent of the form of $b(\theta)$.

V. CONCLUSIONS

We have demonstrated that every two-dimensional rigid body making elastic collisions between parallel walls is equivalent to a traditional billiard problem in which a point particle makes specular reflections with walls of uniquely determined shape. Certain shapes of particular geometrical interest may encourage the consideration of specific billiard problems which might otherwise have escaped attention. Rectangles and shapes of constant width may warrant investigation. Strongly asymmetric rigid bodies strike us as being of particular interest. We note that the present results can be extended to include the effects of external fields.

Similarly, every such billiard problem can be associated with a family of equivalent rigid body problems. This offers the possibility of viewing the extensive billiard literature in a new and potentially revealing light. This equivalence can be extended. It is evident, for example, that similar results can be obtained for a two-dimensional body confined in a rectangular box. There is, of course, nothing to preclude the consideration of billiard problems in higher dimensional spaces. We believe that the existence of simple physical systems can give such systems an intuitive immediacy which they might otherwise lack. Also, the motion of a rigid body in three and higher dimensions is associated with a noncommutative group. Thus, we expect it to be equivalent to a new type of billiard motion.

Finally, the analogous quantum-mechanical problem of rigid bodies confined between parallel walls is of evident interest and is a current focus of our attention. Here, the features of the quantal results require a new interpretation, due to the new association with a different physical property, the tunneling from heads to tails.

ACKNOWLEDGMENTS

We would like to acknowledge helpful discussions with Dr. Serge Troubetzkoy. One of us (R.C.) would like to acknowledge helpful discussions with M. Khanji. This work was supported in part by the U.S. Department of Energy under Grant No. DE-FG02-88ER 40388 (A.D.J. and R.C.) and by the National Science Foundation (N.L.B.).

APPENDIX

Here we shall start from the wall shape obtained for an elliptic disk and consider the various rigid body shapes

which result from different choices of b_0. Specifically, we take

$$b(\theta) = b_0 + \left[\frac{1+\epsilon\cos^2\theta}{1+\epsilon}\right]^{1/2} . \quad \text{(A1)}$$

In the vicinity of $\alpha = 0$, we find

$$R(\alpha) = (b_0+1) - \frac{1}{2}\,\frac{(1+b_0)\epsilon}{1+b_0(1+\epsilon)}\,\alpha^2 + \cdots . \quad \text{(A2)}$$

It is useful to recall that the curvature of $R(\alpha)$ is

$$K(\alpha) = \frac{R^2 + 2R'^2 - RR''}{(R^2+R'^2)^{3/2}}, \quad \text{(A3)}$$

where primes indicate derivatives with respect to α. The curvature corresponding to Eq. (24) at $\alpha = 0$ is thus

$$K(0) = \frac{1+\epsilon}{1+b_0(1+\epsilon)} . \quad \text{(A4)}$$

Evidently, there is a critical value of b_0, $b_c = -1/(1+\epsilon)$ such that $K(0)$ is negative for $b_0 < b_c$. Since the wall function was assumed to come from the convex hull of the original rigid body, this result is unphysical. There is no corresponding rigid body for $b_0 < b_c$. It is instructive to describe what happens as one integrates from $\alpha = \pi/2$ to $\alpha = 0$ in order to obtain $R(\alpha)$.

Case I ($b > b_c$). Here, $R(\alpha)$ approaches b_0+1 quadratically (as expected) and $R'(\alpha)$ approaches 0 linearly as $\alpha \to 0$. The result is a physical shape which depends on b_0. The result is consistent in the sense that the original wall function can be reconstructed from this $R(\alpha)$ using the general prescription of Sec. II.

Case II ($b = b_c$). This is the limiting physical case. Now, $R(\alpha)$ approaches $b_0 + 1$ like $\alpha^{4/3}$ and $R'(\alpha)$ goes like $\alpha^{1/3}$. Clearly, R'' is badly behaved at $\alpha = 0$, but this causes no difficulty. Again, the result is a completely physical shape which permits reconstruction of the original wall function. This critical shape is shown in Fig. 4.

Case III ($b < b_c$). $R(\alpha)$ approaches b_0+1 *linearly*, but $R'(\alpha)$ does *not* approach 0. Rather, it approaches some nonzero value, R'_0, linearly. The putative shape has a discontinuous derivative at $\alpha = 0$ (and $\alpha = \pi$). To see what this means, return to Eq. (12). The range $0_+ < \alpha \le \pi/2$ corresponds to covering the range $\theta_c \le \theta \le \pi/2$

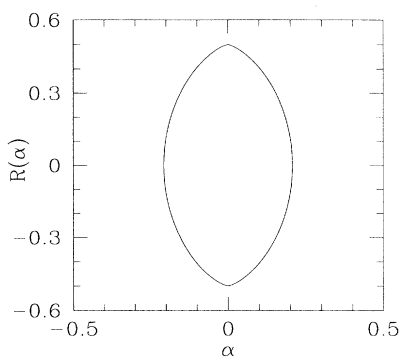

FIG. 4. The rigid body shape ($\vec{R}(\alpha)$) corresponding to the limiting physical case of $b_0 = b_c = -1/2$, ($\epsilon = 1$).

with

$$\theta_c = \tan^{-1}\left(\frac{R'_0}{(b_0+1)}\right) . \quad \text{(A5)}$$

The finite region between $-\theta_c < \theta < +\theta_c$ is all governed by the infinitesimal region $0_- < \alpha < 0_+$. There is nothing wrong with a single point on the body determining the wall shape for a finite angular interval. This occurs whenever the rigid body has a corner and $R(\alpha)$ has a discontinuous derivative. However, as in Eq. (5), this should correspond to a shape $(b_0+1)|\cos\theta|$. Evidently, this is not the shape of $b_0 + b(\theta)$ chosen here nor will it be for other choices of $b(\theta)$. Hence, the resulting body shape will fail to reproduce $b_0 + b(\theta)$ over the range $-\theta_c < \theta < \theta_c$, and thus $R(\alpha)$ is not acceptable. We remark that, in the present example, $b_0 + b(\theta)$ remains positive (and thus not manifestly unphysical) for values of b_0 as small as $-1/\sqrt{1+\epsilon}$, which is less than the limiting value of b_c quoted above.

Similar estimates on b_c based on the existence of regions of negative curvature at the extrema of $b(\theta)$ can be made for arbitrary (differentiable) wall functions since these extrema necessarily coincide with the extrema of $R(\alpha)$. Negative curvature always indicates an unphysical shape. While we have not demonstrated that the first appearance of negative curvature will be at an extremum, the ease of these estimates suggests that they may be useful.

[1] G. Gallavotti and D. Ornstein, Commun. Math. Phys. **38**, 83 (1974); N. Chernov, Ergod. Theor. Dynam. Syst. (to be published).
[2] Ya.G. Sinai, Russ. Math. Surveys. **25**, 137 (1970).
[3] L.A. Bunimovich, Commun. Math. Phys. **65**, 295 (1979).
[4] G. Benettin and J.M. Strelcyn, Phys. Rev. A. **17**, 773 (1978).
[5] O. Bohigas and M.J. Giannoni, in *Mathematical and Computational Methods in Nuclear Physics*, edited by J.S. Dehesa, J.M.G. Gomez, and A. Polls, Lecture Notes In Physics Vol. 209 (Springer, New York, 1984).
[6] E. Doron, U. Smilansky, and A. Frenkel, Phys. Rev. Lett. **65**, 3072 (1990).
[7] R.A. Jalabert, H.U. Baranger, and A.D. Stone, Phys. Rev. Lett. **65**, 2442 (1990).
[8] C.M. Marcus, A.J. Rimberg, R.M. Westervelt, P.F. Hopkins, and A.C. Gossard, Phys. Rev. Lett. **69**, 506 (1992).
[9] V.A. Arnold, *Mathematical Methods of Classical Mechanics*, 2nd ed. (Springer Verlag, New York, 1989).
[10] P.L. Garrido and G. Gallavotti, J. Stat. Phys. **76**, 549 (1994).